

Single site double core level ionisation of OCS

L. Hedin¹, M. Tashiro², P. Linusson³, J.H.D. Eland^{1,4}, M. Ehara², K. Ueda⁵, V. Zhaunerchyk^{1,6}, L. Karlsson¹, and R. Feifel^{1,6*}

¹Department of Physics and Astronomy, Uppsala University, 751 20 Uppsala, Sweden

²Institute for Molecular Science, Nishigo-Naka 38, Myodaiji, Okazaki 444-8585, Japan.

³Physics Department, Stockholm University, 106 91 Stockholm, Sweden

⁴Department of Chemistry, Physical and Theoretical Chemistry Laboratory, Oxford University, South Parks Road, Oxford OX1 3QZ, United Kingdom

⁵Institute for Multidisciplinary Research for Advanced Materials, Tohoku University, Sendai 980-8577, Japan.

⁶Department of Physics, Gothenburg University, 412 96 Gothenburg, Sweden

*corresponding author: raimund.feifel@physics.gu.se

Abstract

Single site O1s, C1s and S2p double ionisation of the OCS molecule has been investigated using a magnetic bottle multi-electron coincidence time-of-flight spectrometer. Photon energies of 1300 eV, 750 eV and 520 eV, respectively, were used for the ionisation, and spectra were obtained from which the double core ionisation energies could be determined. The energies measured for 1s double ionisation are 1172 eV (O1s⁻²) and 659 eV (C1s⁻²). For the S2p double ionisation three dicationic states are expected, ³P, ¹D and ¹S. The ionisation energies obtained for these states are 373 eV (³P), 380 eV (¹D) and 388 eV (¹S). The ratio between the double and single core ionisation energies are in all cases equal or close to 2.20. Auger spectra of OCS, associated with the O1s⁻², C1s⁻² and S2p⁻² dicationic states, were also recorded incorporating both electrons emitted as a result of the filling of the two core vacancies. As for other small molecules, the spectra show an atomic-like character with Auger bands located in the range 480 - 560 eV for oxygen, 235 - 295 eV for carbon and 100 - 160 eV for sulphur. The interpretation of the spectra is supported by CASSCF and CASCI calculations. The cross section ratio between double and single core hole creation was estimated as $3.7 \cdot 10^{-4}$ for oxygen at 1300 eV, $3.7 \cdot 10^{-4}$ for carbon at 750 eV and as $2.2 \cdot 10^{-3}$ for sulphur at 520 eV.

Introduction

Single core ionisation of matter has been extensively studied and electron binding energies and photoionisation cross-sections have been determined for numerous atoms and molecules. Several books have been written on the subject including the two ESCA (Electron Spectroscopy for Chemical Analysis) books from the 1960's [1,2]. Double (and multiple) core ionisation is less well known, and data for atoms and molecules are still rather sparse, since such investigations are much more difficult to carry out experimentally. It is with the advent of highly efficient coincidence methods for electron detection that such studies have become possible in a systematic manner.

This study of double photoionisation of the OCS molecule aims at providing some fundamental data on the core level electronic states as well as on secondary processes occurring upon the creation of the highly excited dicationic states. The electron configuration of the neutral ground state of OCS may in this perspective be written (following electron binding energies)

$S1s^2 O1s^2 C1s^2 S2s^2 S2p^6$ (inner valence shells)(outer valence shells).

The inner shell orbitals involved in the study are essentially atomic-like and we therefore use atomic labels for characterization as is generally done in such cases, and has been done particularly in recent studies of the NO and N₂O [3] and NH₃, CH₄ and H₂CO [4] molecules. The investigation incorporates all the "core orbitals" except S1s, for which the synchrotron radiation photon energy range available was insufficient for double photoionisation. Multi-electron coincidence data have been obtained from which double core ionisation energies have been determined, and comparisons with the corresponding single core ionisation energies are made. In all cases except for the S2p shell a single electronic state arises upon double ionisation. For S2p three dicationic states, ³P, ¹D and ¹S, (using the atomic labels), are expected.

The secondary processes, in which the inner shell holes are filled by electrons from outer shells, release additional electrons in Auger transitions. These electrons are detected as well, and are used to derive associated Auger spectra by coincidence analysis. In the method used, four electrons were detected in coincidence, two fairly slow electrons from the photoionisation process, and two fast Auger electrons. The

photoelectrons were relatively slow because the photon energies were chosen near the double ionisation limit. Generally, they share the available energy arbitrarily which is frequently found to be unequally, where one electron takes a higher and the other a lower energy.

The Auger processes are labeled as in previous studies as DCH \rightarrow CVV (first transition) and CVV \rightarrow VVVV (second transition). DCH means double core hole state, CVV means a state carrying one core hole and two valence vacancies, and VVVV means four vacancies in the valence region.

To provide theoretical support for the interpretation of the Auger spectra, CASSCF (complete active space self-consistent field) and CASCI (configuration interaction) calculations were performed of the Auger kinetic energies and intensities using a theoretical procedure as described previously for calculations of related Auger spectra in Refs. [3,4].

Experimental details

The experimental studies were carried out at the soft-X-ray undulator beamline U49/2 PGM-2 at the electron storage ring BESSY-II in Berlin using the previously described Time-Of-Flight PhotoElectron-PhotoElectron COincidence (TOF-PEPECO) technique [5,6], which is based on the ‘magnetic bottle’ principle [7]. Briefly, photoionisation occurs in the region where an effusive target gas jet from a hollow needle of about 1 mm inner diameter crosses the photon beam in the presence of a strong magnetic field produced by a permanent magnet giving a divergent field of approximately 0.7 T. This field reflects and directs almost all emitted electrons into a 2.2 m long flight tube, where they follow the homogeneous field lines of a weak (10^{-3} T) solenoid. The Lorentz force causes the emitted electrons to spiral around these magnetic field lines up to the end of the flight tube, where they impinge on a microchannel plate detector containing three plates in Z-stack configuration.

After discrimination, the electron signals are recorded by a multi-channel, multi-hit, time-to-digital converter card in a local computer. The converter also registers timing signals from the storage ring. The storage ring was operated in single bunch mode,

which provides 30 ps light pulses at an inter-pulse spacing of 800.5 ns [8]. In this mode of operation the energy resolution for single electrons can numerically be approximated as one part in 50 of the electron energy.

Each single photon may lead to the ejection of 4 electrons, two electrons from the primary process that gives rise to the double core holes, and two fast electrons from secondary Auger transitions where valence electrons fill the core vacancies. This process mostly leads to final states with four vacancies in the valence electronic shells. In order to reduce the number of accidental coincidences the total electron count rate was limited to about 1.3 kHz, compared with a light-pulse repetition rate of 1.25 MHz. To increase the reliability of the data, we have, in the data extraction and determination of kinetic energies, used only coincidence events where in each case all four emitted electrons were identified.

The measured flight times are related to the kinetic energies by the formula [5]

$$E = \frac{D^2}{(t - t_0)^2} - E_0$$

D contains the fixed flight length and E_0 and t_0 are calibration parameters taking into account instrumental offsets in energy and flight-time, respectively. In the present investigation they were obtained from known energies of the xenon atom, for which spectra were recorded separately. The parameter values were obtained as: $D = 3700$ ns $\sqrt{\text{eV}}$; $E_0 = 0.37$ eV; $t_0 = 23.9$ ns.

The sample gases were obtained commercially with a stated purity of > 99.6 %. The purity was checked throughout the studies by recordings of photoelectron spectra.

Theoretical details

Auger spectra were calculated as based on the two-step Auger decay mechanism of the DCH state previously described in Ref. [4]. The energies of the DCH, CVV and VVVV states were obtained by the full-valence complete active space configuration interaction (CASCI) method based on the state-averaged complete active space SCF (CASSCF) [9,10] molecular orbitals (MOs).

The relative Auger intensities were evaluated using Wenzel's formula with the full-valence CASCI wave functions of the DCH, CVV and VVVV states. The two-electron integrals involving the Auger electron orbital were approximated using the population of MOs [4,11]. Further detail of the calculation procedure is described in Ref. [4].

The energies and wave functions of the DCH, CVV, and VVVV states were evaluated at the experimental equilibrium geometries of the neutral OCS molecule [12]. We used C_{2v} symmetry in the calculations, although the geometries of this molecule correspond to $C_{\infty v}$ symmetry. The cc-pVTZ basis set [13] was employed. As active orbitals in the CASSCF and CASCI calculations, we used a total of 12 valence orbitals for the OCS molecule. Important orbitals such as σ , σ^* , π , and π^* are all included in this active orbital space. The $O1s$, $C1s$, $S1s$, $S2s$ and $S2p$ core orbitals were kept frozen during all the CASSCF orbital optimizations, using those obtained by the Hartree–Fock calculation on the neutral molecule. Spin-orbit interaction was not considered in this work. For each of the $O1s^{-1}$, $C1s^{-1}$, and $S2p^{-1}$ CVV states, 12000 doublet states were calculated by the CASCI method. The MOs were obtained by the CASSCF calculations with state averaging over the lowest 8, 11 and 14 electronic states for the $O1s^{-1}$, $C1s^{-1}$, and $S2p^{-1}$ CVV states, respectively. For the VVVV states, 18000 singlet states and 18000 triplet states were obtained by the CASCI calculations. The state-averaged CASSCF calculations were performed for the lowest 8 states both for the singlet and the triplet spin multiplicities. Auger intensities were calculated for all the possible DCH-CVV transitions, i.e., 12000 transitions for each DCH decay. For the CVV-VVVV Auger transitions, the CVV states having finite DCH-CVV Auger intensities were selected, and then Auger intensities were calculated for all the possible pairs of CVV and VVVV states. For example, in the case of the $O1s^{-2}$ DCH decay, Auger intensities were calculated for 5760000 transitions in the CVV-VVVV Auger decay, although only a small fraction of these transitions contributes to the total Auger intensity. For the initial electronic state of the $S2p^{-2}$ DCH Auger decay, we selected the $1^1\Delta$ state, one of the three electronic states ($1^1\Delta, 1^1\Sigma$ and $1^1\Pi$) derived from the atomic 1^1D state.

The CASSCF calculations were performed using the MOLPRO program package [14], while the SCATCI module in the UK R-matrix codes [15] was used for the CASCI calculations.

Results and discussion

Time-of-flight coincidence spectra associated with double core ionisation of the OCS molecule have been recorded using the apparatus described in the experimental section. These spectra show the total coincidence intensity as a function of the sum of the energies of the two electrons emitted in the primary process initiated by the incident photon. The double ionisation energies, DIE, are given in Table 1. For the purpose of systematic comparison, the corresponding single ionisation energies, denoted IE and taken from Refs. [16,17], are included in Table 1 along with the ratio between double and single ionisation energies. In addition, the data can be plotted in form of maps, which show the coincidence counts as a function of the kinetic energies of either of the two core electrons liberated by the incident photon. An example of such a map is shown below in Fig. 4 along with the corresponding spectrum for the S2p double ionisation of OCS shown in Fig. 3.

Fig. 1 shows the O1s double core hole spectrum of the OCS molecule recorded using the photon energy 1300 eV. It reveals one single line at the binding energy 1172 eV, whereas the calculated energy is 1168.5 eV. The experimental value was obtained as the energy difference between 1300 eV and the sum of the kinetic energies of the two emitted photoelectrons, 128 eV. The DIE is thus found to be 2.17 times the energy for O1s single ionisation (540.28 eV) [16], which is very close to the ratio between DIE and IE of core levels obtained for other small molecules [3]. A similar increase in ionization energy has been found for small molecules also when comparing valence energies, but in these cases a correction is needed for the Coulomb interaction between the delocalized holes [18]. The value of 2.17 is in fact the same as was obtained for the oxygen atom of the NO and N₂O molecules [3]. In both double and single ionisation, the O1s binding energy is lower for OCS than for NO and N₂O. This can be understood in terms of the lower electronegativity of both carbon and sulphur than for the nitrogen atom. The results also reinforce previous observations and

predictions [3, 4, 19 - 22] that chemical shifts are systematically larger for doubly ionised than singly ionised core hole states.

As concerns chemical shifts it is interesting to compare with the O1s IE and DIE of the O₂ molecule, 543.86 eV [23] (weighted average of the ⁴Σ and ²Σ states) and 1179.2 ± 0.8 eV [24], respectively. These comparatively high binding energies reflect the larger electronegativity of the oxygen atom than for C, N and S. The shifts of OCS compared to O₂ are 3.58 eV (IE) and 7.2 eV (DIE); i.e. the shift in double ionisation is here 2 times that of single ionisation.

Another observation is that in the O1s spectrum the well-defined line is accompanied by an underlying broad structure. Much of the intensity is attributed to accidental coincidences with possible contributions of shake-up and shake-off processes in the double ionisation.

Fig. 2 shows the double ionisation C1s spectrum of the OCS molecule using the photon energy 750 eV. The C1s double core ionisation is represented by a sharp line in the spectrum. The DIE determined from this line in a similar way as for O1s is 659 eV, whilst the calculated energy is 657.7 eV. The corresponding experimental C1s single core ionisation energy (IE) is 295.43 eV [16], which means that the ratio between the double and single core ionisation energies is in this case 2.23. This value differs marginally from 2.17 obtained for the oxygen atom, but a closer inspection of the ratio DIE/IE shows that there are small but characteristic differences between the atoms. In particular, for the molecules OCS, O₂, NO and N₂O the value is 2.17 for the O1s ratio, 2.20 for the N1s ratio and 2.23 for the C1s ratio. As suggested in Ref. [4], the differences can be explained in terms of the electronegativity and hence the reorganization of the electronic structure upon ionisation.

Another observation in the C1s spectrum is a background which origin is similar to the O1s spectrum. I.e. it is primarily related to the large number of low energy electrons with random energies moving around in the apparatus.

In the corresponding coincidence map (not presented here) connected to the formation of the C1s⁻² dication in its ground electronic state a clear straight line between the axis points at 91 eV (750 – 659 eV) is observed. A large number of accidental coincidences can be seen also in this case. In particular, they seem to be located

primarily close to the axes, which means that the two electrons have widely different energies.

Fig. 3 shows the double ionisation S2p spectrum of the OCS molecule using the photon energy 520 eV. The double ionisation leads, in this case, to three final states associated with the $S2p^{-2}$ electron configuration. In the spectrum, two well defined lines are observed at 373 eV and 380 eV, respectively. We assign these to the 3P and 1D states of the dication. The third state to be expected, 1S , is most likely reflected by the line at 388 eV. This line is less well resolved though, and of the same relative intensity as the structures of the accompanying intensity due to the presence of background, so this assignment is less certain. However, in the spectrum of SF_6 (cf. Ref. [25]), the corresponding line is much better resolved from the background, and for this case the assignment is obvious, as also from a comparison with recently published spectra of H_2S , SO_2 and CS_2 [21]. The theoretical energies are a few eV higher than the experimental values (cf. Table 1), but the energy separations are similar and thus also support the assignments.

The energy separations of 7 eV (3P - 1D) and 8 eV (1D - 1S) obtained with this interpretation are similar to the corresponding separations reported for the $2p^{-2}$ states of the argon dication [26- 28]. This difference can be explained by the higher atomic number of argon than of sulphur.

Using weighted averages of the multiplet states for the DIE, 376 eV, and the IE, 171 eV, the ratio DIE/IE is similar to that of the other atoms, 2.20. This strengthens the interpretation of the S2p orbital as primarily atomic like.

It has been observed also in many other cases (e.g. Ref. [21,28]), that the relative intensities between the 3P , 1D and 1S final states disagree drastically from the statistical ratio of 9:5:1. In particular, the observed line corresponding to 3P is much weaker than expected from these figures. As mentioned in Refs. [21,28], simple statistical arguments may not be sufficient to explain the behaviour, and further theoretical investigations are suggested. However, it may be rationalised in a simplistic manner, if the second electron is assumed to leave the system due to a classical-like collision with the photoelectron. The probability that the photoelectron hits an electron with the same spin in the same 2p shell is then 2/5 whereas it is 3/5

for the opposite spin. There is thus 40 % chance to create a triplet state in the dication and 60 % chance of creating a singlet state, which is at least qualitatively in fair agreement with the experimental spectrum.

Fig. 4 shows the corresponding coincidence map where each data point is defined by the kinetic energies of the two electrons, e_1 and e_2 , separately represented on the horizontal and vertical axis, respectively. As can be seen, coincidences associated with the total kinetic energy sum of 140 eV and 147 eV form two clear straight lines between the points on the horizontal and vertical axes with this energy.

Some of the data points in Fig. 4 correspond to kinetic energies much larger than the maximum energy, 147 eV, and they are clearly associated with accidental events. Some of the data points inside the “energetically allowed” region may also be due to such accidental events, but true coincidences in this region are expected to be present due to shake-up and shake-off processes.

At 1300 eV photon energy the ratio of fourfold coincidences from DCH formation to twofold coincidences from single core hole formation at the O atom was $9.2 (\pm 0.2) \cdot 10^{-5}$. In view of the measured collection efficiency of about $0.5 \pm .05$, assumed to be independent of electron energy over the range involved, this implies a cross-section ratio between double and single ionisation of $3.7 (\pm 0.2) \cdot 10^{-4}$ at this photon energy. Similarly the estimated cross-section ratio is for the C atom $3.7 (\pm 0.2) \cdot 10^{-4}$ at 750 eV photon energy and for the S atom $2.2 (\pm 0.2) \cdot 10^{-3}$ at 520 eV. Because the true collection efficiency is likely to be lower for the high energy photoelectrons from SCH formation, these ratios should be taken as upper limits.

The OCS Auger electron spectrum

Figure 5 shows an Auger electron spectrum of OCS recorded using the photon energy 1300 eV for the creation of the initial O1s core holes. It exhibits two broad features centred at about 560 eV and 480 eV, which is very similar to the corresponding spectrum of N₂O [3] and that predicted for H₂CO [4]. The former energy is clearly associated with DCH → CVV and the latter with CVV → VVVV processes. The theoretical spectrum, also shown in this figure, is in good agreement showing

intensity maxima at 570 eV and 490 eV. The calculations were performed using the CASSCF and CASCI methods as described in the theoretical section above and previously [3,4].

Many different final electronic states can be formed by combination of four valence holes, and all these states are expected to contribute at well-defined energies to the spectrum of Fig. 5. The hole states may involve vacancies distributed in various ways in both the outer and inner valence regions, which explains the large width of each feature, and the energies of 560 eV and 480 eV represent rather average energies for all transitions. The DCH state is single so in the DCH \rightarrow CVV case of the structure in the spectrum has the width associated with the available CVV states. For the CVV \rightarrow VVVV case the spectral distribution is a reflection of all the CVV and VVVV states. From these data average energies for the CVV and VVVV states can be estimated as 610 eV (CVV) and 130 eV (VVVV).

Figure 6 shows an Auger electron spectrum of OCS recorded using the photon energy 750 eV for the creation of the initial C1s double core holes. As for the O1s⁻² case, two broad features are observed. They are centred at about 300 eV and 240 eV and clearly associated with DCH \rightarrow CVV and CVV \rightarrow VVVV processes, respectively. Also in this case the theoretical spectra are in good agreement showing peak maxima at about 310 eV and 245 eV. The energies are essentially the same as found for the C1s⁻² initial state of the H₂CO molecule [4], which gives further support for the previous suggestion [3] that spectra of this kind are useful for elemental analysis. In all cases, the structures have a comparatively large width reflecting transitions involving a large number of valence states, but the mean energy of the structures is characteristic of the atom carrying the initial double vacancy. Like for the oxygen case, average energies for the CVV and VVVV states can be estimated as 360 eV (CVV) and 120 eV (VVVV). The latter value is rather similar to that of the O1s⁻² case, as expected. The difference of 10 eV is due to both the uncertainty in the average energies and different transition probabilities in the two cases.

Figure 7 shows an Auger spectrum obtained for S2p double ionisation. Two broad bands can be discerned, as for O1s and C1s, which correspond to the DCH \rightarrow CVV and CVV \rightarrow VVVV processes. The structures are more complex than for the oxygen

and carbon cases, since there are three initial dicationic states, 3P , 1D and 1S . Furthermore, the CVV state is split into two components by spin-orbit coupling of the S2p orbital. It is thus not easy to estimate an average energy associated with the VVVV configuration, but it is located in the interval between 110 eV and 130 eV.

Figure 8 shows an energy level diagram and the transitions and various charge states involved in the Auger processes associated with O1s, C1s and S2p double ionisation. The energies for the singly and doubly charged states are accurate and associated with well defined individual spectral lines, whilst the energies given for the more highly charged states and transitions are estimated average values.

Conclusions

O1s, C1s and S2p core level double ionisation has been studied experimentally using a coincidence detection technique based on flight time measurements. The double ionisation energies were found to be 1172 and 659 eV for O1s and C1s, respectively. For S2p double ionisation three final states can be reached, 3P , 1D and 1S . The energies for these are found to be 373 eV, 380 eV and 388 eV, respectively. The ratio between the double (DIE) and single (IE) ionisation energies is found to be remarkably similar in all cases, 2.17 for O1s, 2.20 for S2p and 2.23 for C1s. The ratios are similar to the corresponding values for these atoms in other molecules confirming the strong atomic nature of the inner shell electrons. The DIE and IE were calculated using CASSCF and CASCI methods. The energies were found to be close to the experimental values as well as the ratios DIE/IE.

Auger spectra were recorded of the electrons released as a result of the filling of the core holes. Also in these cases, the atomic nature of the processes was striking. The filling of the first hole gave an Auger electron with an average kinetic energy of 560 eV for O1s, 295 eV for C1s and 150 eV for S2p. The corresponding kinetic energies associated with the filling of the second hole were 480 eV, 245 eV and 100-120 eV, respectively. CASSCF and CASCI calculations gave results in good agreement with the experimental data.

Acknowledgement

This work has been financially supported by the Swedish Research Council (VR) and the Knut and Alice Wallenberg Foundation, Sweden. M.E. and M.T. acknowledges the support from a Grant-in-Aid for Scientific Research from the Japan Society for the Promotion of Science (JSPS). KU acknowledges MEXT for support on the X-ray Free Electron Laser Utilization Research Project, on the X-ray Free Electron Laser Priority Strategy Program, and on the Research Program of Network Joint Research Center for Materials and Devices. We would like to warmly acknowledge the support by the staff and colleagues at BESSY-II, Berlin. This work was also supported by the European Community - Research Infrastructure Action under the FP6 "Structuring the European Research Area" Programme (through the Integrated Infrastructure Initiative "Integrating Activity on Synchrotron and Free Electron Laser Science" - Contract R II 3-CT-2004-506008).

References

- [1] Kai Siegbahn et al., *ESCA: Atomic, Molecular and Solid State Structure Studied by means of Electron Spectroscopy*, Almqvist & Wiksell, Uppsala, 1967.
- [2] Kai Siegbahn et al., *ESCA applied to Free Atoms and Molecules*, North-Holland Publ. Co, 1969.
- [3] L. Hedin, M. Tashiro, P. Linusson, J.H.D. Eland, M. Ehara, K. Ueda, V. Zhaunerchyk, L. Karlsson, K. Pernestål, and R. Feifel, *J. Chem. Phys.* **140**, 044309 (2014).
- [4] M. Tashiro, K. Ueda, and M. Ehara. *J. Chem. Phys.* **135**, 154307 (2011).
- [5] J.H.D. Eland, O. Vieuxmaire, T. Kinugawa, P. Lablanquie, R.I. Hall, F. Penent, *Phys. Rev. Lett.* **90** 053003 (2003).
- [6] R. Feifel, J.H.D. Eland, L. Storchi, F. Tarantelli, *J. Chem. Phys.* **122** 144309 (2005).
- [7] P. Kruit and F. H. Read, *J. Phys. E* **16** 313 (1983).
- [8] <http://www.bessy.de/>
- [9] P.J. Knowles and H.-J. Werner, *Chem. Phys.Lett.* **115**, 259 (1985).
- [10] H.-J. Werner and P.J. Knowles, *J. Chem. Phys.* **82**, 5053 (1985).
- [11] M. Mitani, O. Takahashi, K.Saito, and S. Iwata, *J. Electron Spectrosc. Relat. Phen.* **128**, 103 (2003).
- [12] CRC Handbook of Chemistry and Physics, 93rd Edition (CRC Press, 2012)
- [13] T.H. Dunning Jr. *J. Chem. Phys.* **90**, 1007 (1989).
- [14] H.-J. Werner, P. J. Knowles, F. R. Manby, M. Schütz, P. Celani, G. Knizia, T. Korona, R. Lindh, A. Mitrushenkov, G. Rauhut, T. B. Adler, R. D. Amos, A. Bernhardsson, A. Berning, D. L. Cooper, M. J. O. Deegan, A. J. Dobbyn, F. Eckert, E. Goll, C. Hampel, A. Hesselmann, G. Hetzer, T. Hrenar, G. Jansen, C. Köppl, Y. Liu, A. W. Lloyd, R. A. Mata, A. J. May, S. J. McNicholas, W. Meyer, M. E. Mura, A. Nicklass, P. Palmieri, K. Pflüger, R. Pitzer, M. Reiher, T. Shiozaki, H. Stoll, A. J. Stone, R. Tarroni, T. Thorsteinsson, M. Wang, and A. Wolf, “Molpro, version 2010.1, a package of ab initio programs,” (2010).
- [15] L.A. Morgan, J. Tennyson, and C.J. Gillan, *Comput. Phys. Commun.* **114**, 120 (1998).
- [16] T.X. Carroll, DE JI, and T.D. Thomas, *J. Electron Spectrosc. Relat. Phenom.* **51**, 471 (1990).

- [17] C.M. Truesdale, D.W. Lindle, P.H. Kobrin, U.E. Becker, et al, J. Chem. Phys. **80**, 2319 (1984).
- [18] R. D. Molloy, A. Danielsson, L. Karlsson, and J. H. D. Eland, Chem. Phys. **335**, 49 (2007).
- [19] N. Berrah, L. Fang, B. Murphy, T. Osipov, K. Ueda, E. Kukk, R. Feifel, P. van der Meulen, P. Salen, H.T. Schmidt, R.D. Thomas, M. Larsson, R. Richter, K.C. Prince, J.D. Bozek, C. Bostedt, S. Wada, M.N. Piancastelli, M. Tashiro, and M. Ehara, Proceedings of the National Academy of Sciences **108**, 16912 (2011).
- [20] P. Salén, P. v.d. Meulen, R.D. Thomas, H.T. Schmidt, M. Larsson, R. Feifel, M.N. Piancastelli, L. Fang, T. Osipov, B. Murphy, N. Berrah, E. Kukk, K. Ueda, J.D. Bozek, C. Bostedt, S. Wada, M. Tashiro, M. Ehara, R. Richter, V. Feyer, and K.C. Prince, Phys. Rev. Lett. **108**, 153003 (2012).
- [21] P. Linusson, O. Takahashi, K. Ueda, J.H.D. Eland, and R. Feifel, Phys. Rev. A **83**, 022506 (2011).
- [22] J.H.D. Eland, M. Tashiro, P. Linusson, M. Ehara, K. Ueda, and R. Feifel. Phys. Rev. Lett. **105**, 213005 (2010).
- [23] A. A. Bakke, A. W. Chen and W. L. Jolly, J. Electron Spectrosc. Relat. Phenom. **20**, 333 (1980).
- [24] P. Lablanquie, F. Penent, J. Palaudoux, L. Andric, P. Selles, S. Carniato, K. Bučar, M. Žitnik, M. Huttula, J. H. D. Eland, E. Shigemasa, K. Soejima, Y. Hikosaka, I. H. Suzuki, M. Nakano and K. Ito, Phys. Rev. Lett. **106**, 063003 (2011).
- [25] R. Feifel et al., to be published 2014.
- [26] L. Asplund, P. Kelfe, B. Blomster, H. Siegbahn and K. Siegbahn, Phys. Scr. **16**, 268 (1977).
- [27] M. O. Krause, Phys. Rev. Lett. **34**, 633 (1975).
- [28] P. Linusson, S. Fritzsche, J.H.D. Eland, M. Mucke, and R. Feifel, Phys. Rev. A **87**, 043409 (2013).

Tables

Table 1. Single (IE) and double core level ionisation energies (DIE) of the OCS molecule. Experimental values of the single core level ionisation energies are taken from Refs. [16,17]. The ratios between the DIE and IE are also given. The ratio for S2p is obtained as the weighted average of the multiplet energies.

Orbital	IE (eV)	State	DIE exp. (eV)	DIE theor. (eV)	Molecular state	Atomic state	DIE/IE exp
O1s	540.28	2S	1172	1168.519		1S	2.17
C1s	295.43	2S	659	657.700		1S	2.23
S2p	171.85	$^2P_{1/2}$	373	377.543	$^3\Sigma$	3P	
				377.746	$^3\Pi$		
S2p	170.65	$^2P_{3/2}$	380	383.618	$^1\Delta$	1D	2.20
				383.977	$^1\Sigma$		
				384.037	$^1\Pi$		
S2p			388	394.503	$^1\Sigma$	1S	

Figure captions.

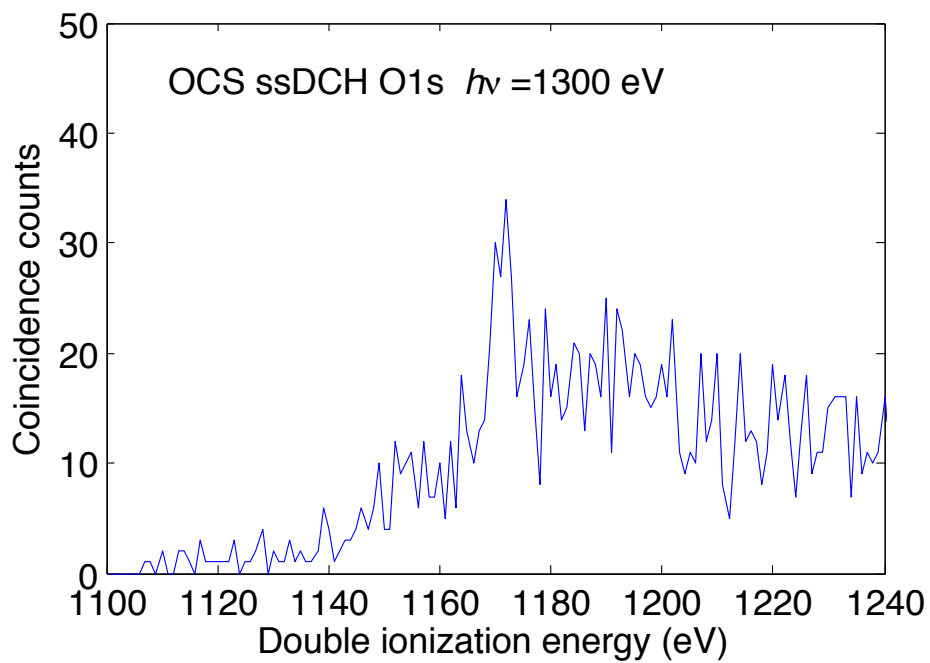


Fig. 1. O1s double core ionisation spectrum of OCS using a photon energy of 1300 eV.

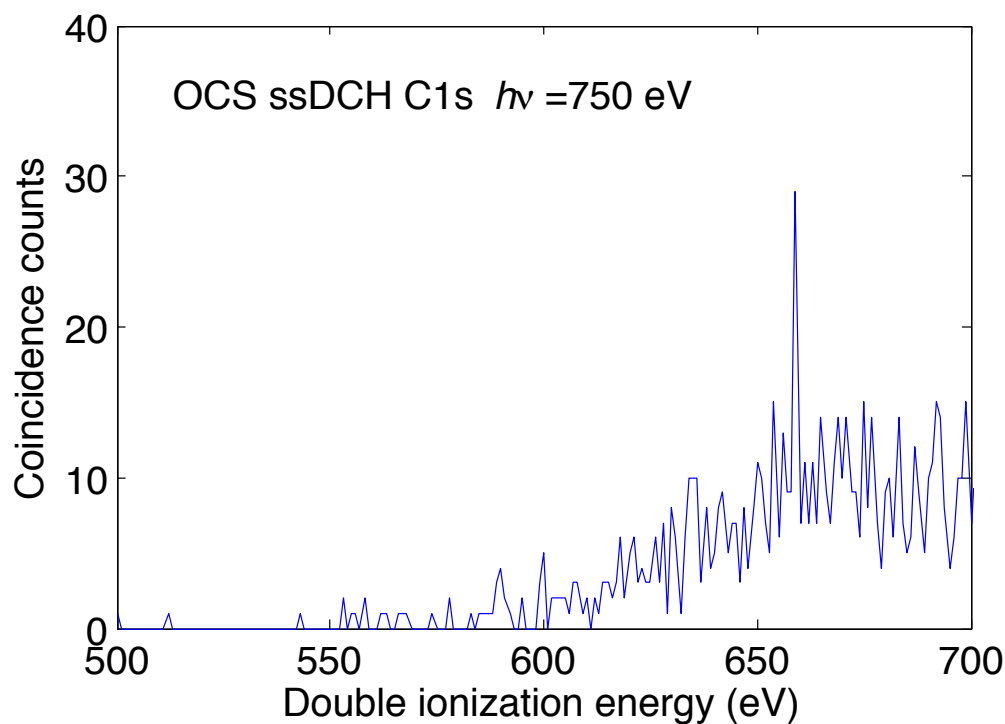


Fig. 2. C1s double core ionisation spectrum of OCS using a photon energy of 750 eV.

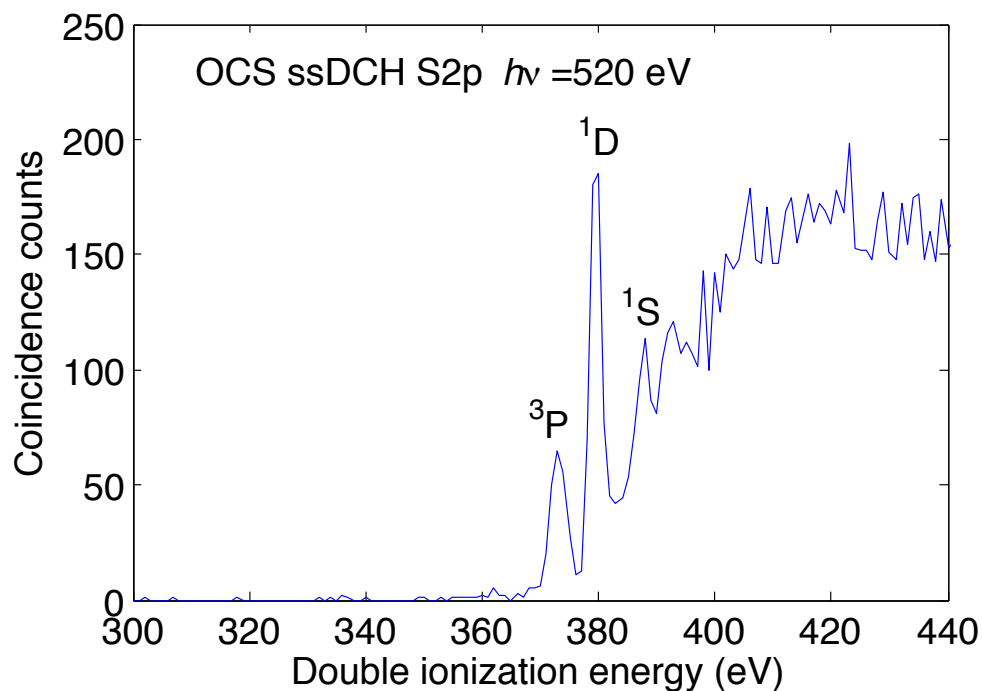


Fig. 3. S2p double core ionisation spectrum of OCS using a photon energy of 520 eV. Three well-defined lines are observed at 373 eV, 380 eV and 388 eV. They are associated with the 3P , 1D and 1S dicationic states, respectively.

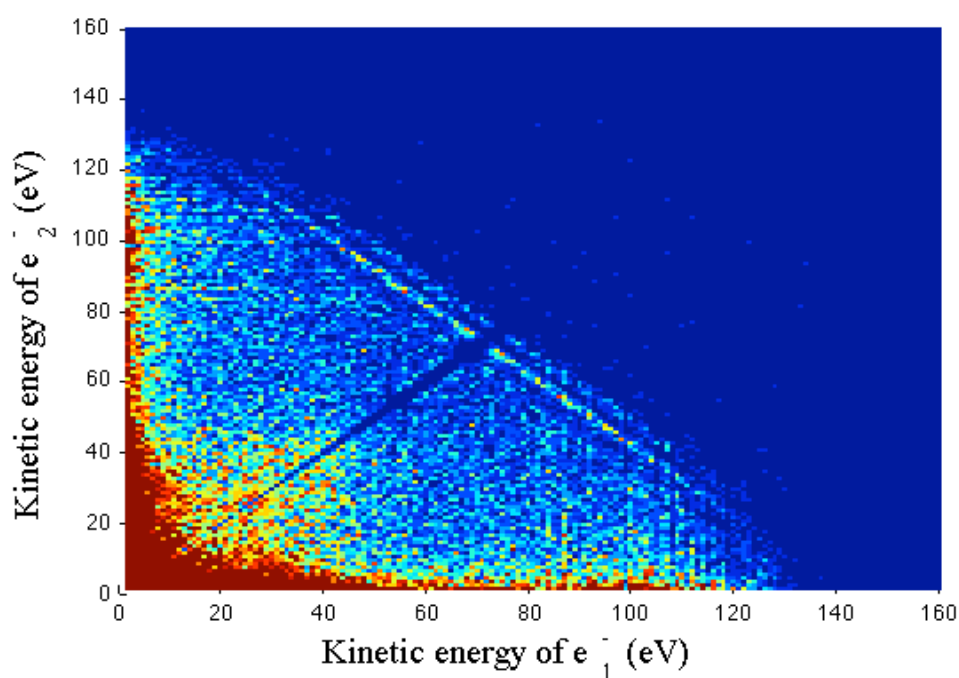


Fig. 4. Intensity map of S2p double core ionisation of OCS using a photon energy of 520 eV. The horizontal and vertical axes represent the kinetic energy of either of the two S2p electrons. The data points lying on a straight line between the points at approximately (0, 147 eV) and (147, 0 eV) as well as the data points lying on a straight line between the points at approximately (0, 140 eV) and (140, 0 eV) correspond to the 3P and 1D dicationic states, respectively.

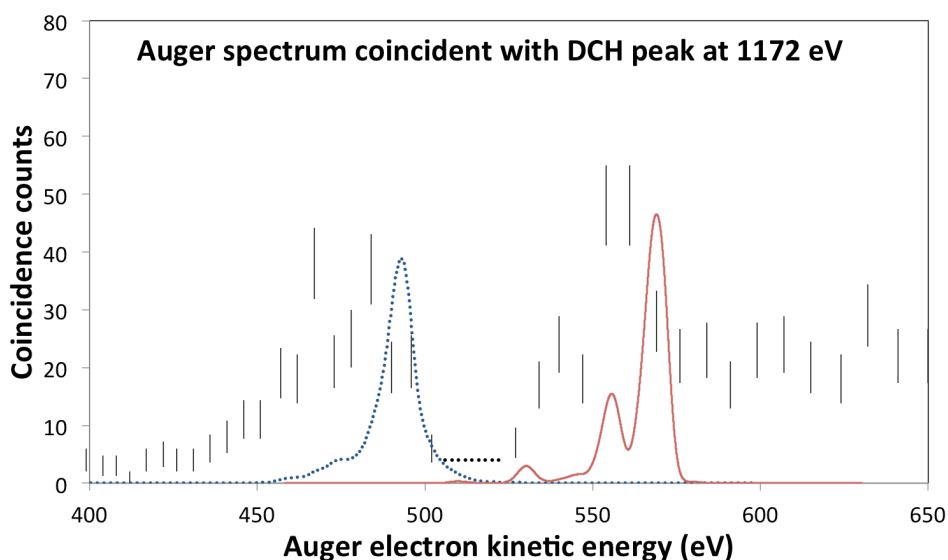


Fig. 5. The Auger electron spectrum of the OCS molecule showing transitions from the double $O1s^{-2}$ inner shell vacancies to final states containing four valence holes.

The photon energy used to create the inner shell vacancies was 1300 eV. The theoretical spectrum is represented by the full line. It was obtained by convoluting each transition with a Gaussian of 5 eV (FWHM) width. The transitions considered are DCH ($O1s^{-2}$) $\rightarrow O1s^{-1}VV$ and $O1s^{-1}VV \rightarrow VVVV$.

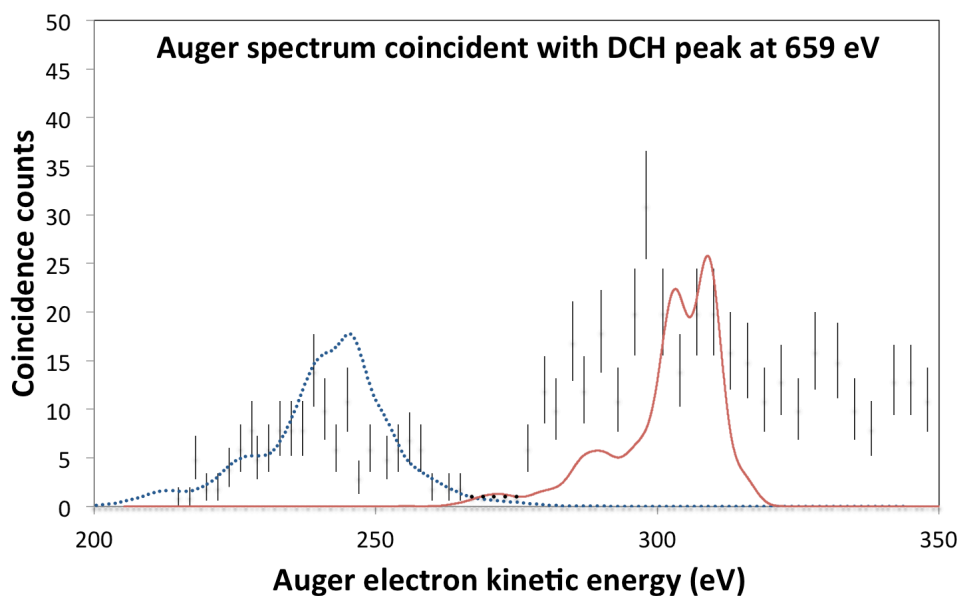


Fig. 6. The Auger electron spectrum of the OCS molecule showing transitions from the double $C1s^{-2}$ inner shell vacancies to final states containing four valence holes. The photon energy used to create the inner shell vacancies was 750 eV. The theoretical spectrum is represented by the full line. It was obtained by convoluting each transition with a Gaussian of 5 eV (FWHM) width. The transitions considered are DCH ($C1s^{-2}$) $\rightarrow C1s^{-1}VV$ and $C1s^{-1}VV \rightarrow VVVV$.

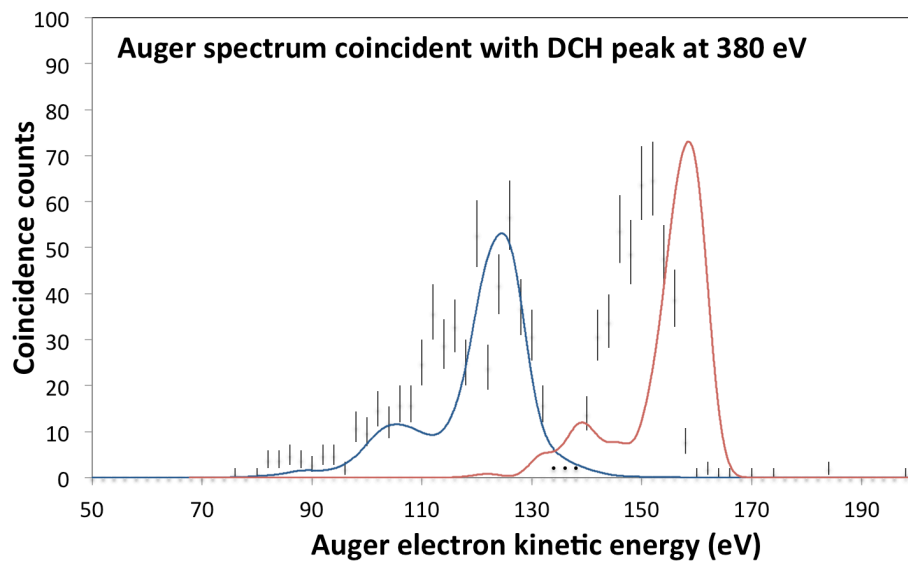


Fig. 7. The Auger electron spectrum of the OCS molecule showing transitions from the $S2p^{-2}$ double inner shell vacancies to final states containing four valence holes. The photon energy used to create the inner shell vacancies was 520 eV. The theoretical spectrum is represented by the full line. It was obtained by convoluting each transition with a Gaussian of 5 eV (FWHM) width. The transitions considered are DCH ($S2p^{-2}$) \rightarrow $S2p^{-1}VV$ and $S2p^{-1}VV \rightarrow VVVV$.

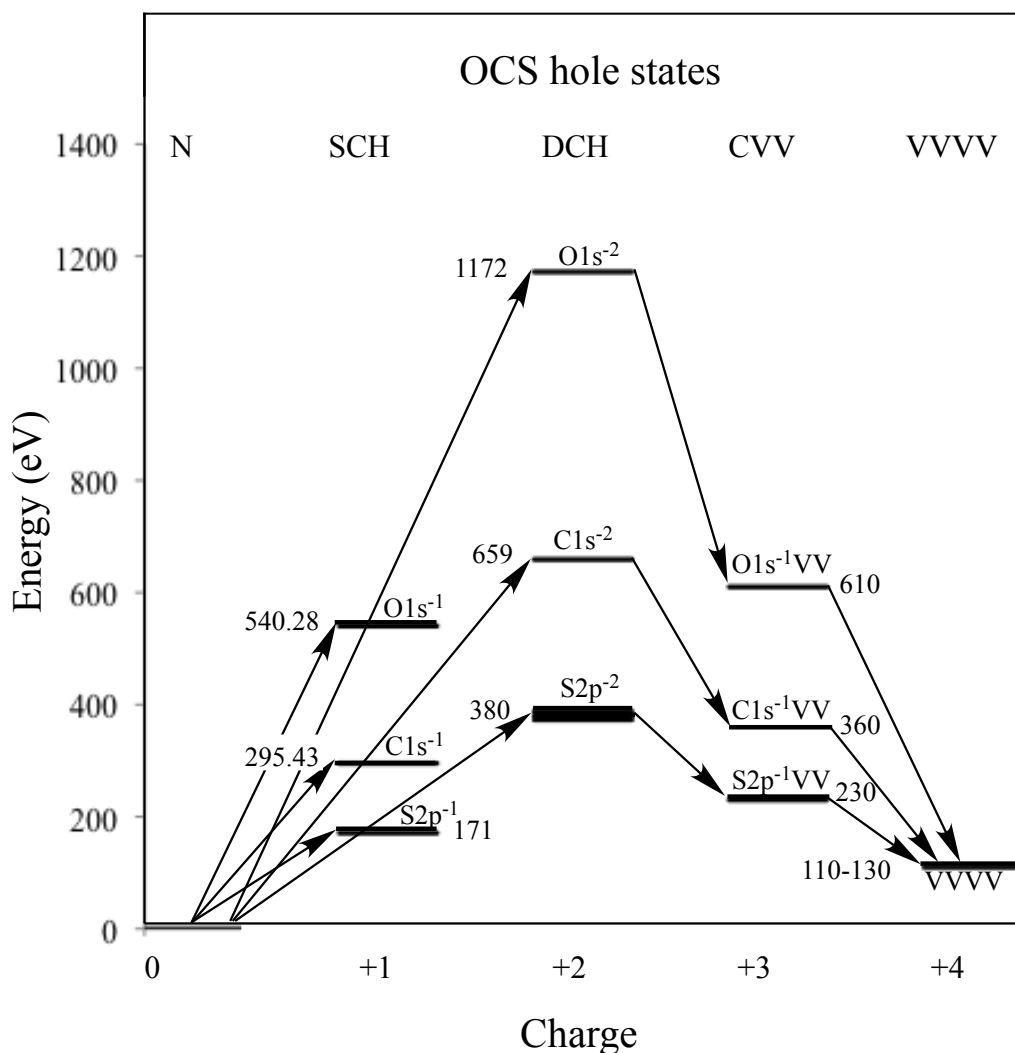


Fig. 8. Energy levels, transitions and charge states involved in the emission of Auger electrons from OCS associated with $O1s^{-2}$, $C1s^{-2}$, and $S2p^{-2}$ inner shell electron configurations. Estimated averages energies are given for the distributions associated with transitions to the CVV and VVVV states.